



The Reggeon Calculus for  $\alpha > 1$

J. B. BRONZAN<sup>\*†</sup>

National Accelerator Laboratory, Batavia, Illinois 60510

and

Rutgers University, New Brunswick, New Jersey 08903

ABSTRACT

We study the Reggeon calculus when Reggeons have  $\alpha(0) > 1$  and vacuum quantum numbers. We sum all the Regge cuts in the weak coupling regime where the  $p$  Reggeon couplings  $r_p$  are small. The resulting amplitude saturates the Froissart bound provided the triple Regge coupling  $r_3$  is dominant. In impact parameter space the amplitude is a uniform absorbing disk whose radius expands like  $\ln s$ . The leading asymptotic term factorizes even when there are arbitrary couplings of the external particles to many Reggeons. In the angular momentum plane the Pomeron is a pair of cuts on the trajectories

$$\alpha_p(t) = 1 \pm 2[\alpha'(\alpha-1)t]^{\frac{1}{2}}.$$

---

\*Research supported in part by the National Science Foundation under grant GP-36740X.



## I. INTRODUCTION

Recent attempts to understand constant or rising cross sections at very high energy show that both the high energy (s) channel and the crossed (t) channels must be carefully treated. In a Regge picture, s channel unitarity leads to strong constraints on the Regge parameters,<sup>1</sup> and t channel processes in which the Reggeon splits into other Reggeons are crucial for the understanding of cuts,<sup>2</sup> and of the couplings that appear in inclusive cross section formulas.<sup>1</sup> Most models shortchange at least one of the aspects of the problem. The result is that they have falling cross sections, or they violate unitarity, or they give absurd formulas for inclusive cross sections in the fragmentation region. In this paper we examine the Reggeon calculus, which emphasizes Reggeon splitting. This type of model is apt to have trouble with unitarity, but in the proper regime we find that s channel unitarity is preserved together with rising cross sections. In our calculations we shall not "force" the Reggeon calculus in any way, but rather evaluate the Reggeon diagrams and take what comes. Since our Reggeons are chosen to have  $\alpha(0) > 1$ , it is close to miraculous that the sum of diagrams just saturates the Froissart bound.

The Reggeon calculus is abstracted from field theory, and in a full calculation the Regge parameters would be determined in terms of masses and couplings of the underlying field theory. If the Regge

parameters are related as the field theory specifies, we expect s channel unitarity to be satisfied. When the field theory is adjusted so that the Reggeons have  $\alpha(0) - 1 \equiv \Delta < 0$ , s channel unitarity in fact says very little, and the various Regge couplings can be chosen arbitrarily, disregarding the relations specified by the field theory. The main point we shall establish in this paper is that, subject to very simple constraints, the Regge parameters can also be chosen arbitrarily for  $\Delta > 0$ , despite the fact that each individual Regge cut badly violates unitarity. It is surprising that the constraints we find should be simple because delicate cancellations are required for the sum of the cuts to satisfy the Froissart bound. The sum of the cuts has the further attractive feature that its form is both simple and independent of the specific field theory used to derive the Reggeon calculus. Contrary to initial expectations, the underlying field theory can be discarded for  $\Delta > 0$ , just as it can for  $\Delta < 0$ . Gell-Mann has compared this process to a method employed in French cuisine: a piece of pheasant meat is cooked between two slabs of veal, which are then discarded.<sup>3</sup>

In this paper we only investigate the asymptotic behavior of four particle amplitudes. It remains to be seen whether the requirements imposed by s channel unitarity on inclusive processes are trivially satisfied for  $\Delta > 0$ . If they are, the Reggeon calculus constitutes a model which is soundly based dynamically, puts all t channels on the same footing, and satisfies s channel unitarity besides. This is an

attractive possibility for the following reason: We know that cuts must play a dominant role in inclusive processes if cross sections do not fall with energy.<sup>1</sup> However, an inclusive amplitude with dominant cuts cannot be parametrized uniquely, so a model is required even for data fitting.

The final Regge singularity we find for  $\Delta > 0$ --hereafter called the Pomeranchon--is an uniform absorbing disk in impact parameter space whose radius grows like  $y = \ell ns$ . Our Pomeranchon differs from that of the Regge-eikonal model<sup>4</sup> because it is gray rather than black, and because cross sections obey factorization relations rather than approaching a common value. The Regge-eikonal black disk can be obtained by choosing special values of the Regge couplings in our model.

A theory with a vacuum Regge pole at  $\Delta > 0$  has a chance of being unitary only if all the attendant Regge cuts are summed. We shall consider a Regge pole on the linear trajectory  $\alpha(t) = \alpha(0) + \alpha't$ . This pole, together with its cuts, leads to the multiple scattering series for the amplitude

$$M(s, t) = \sum_{n=1}^{\infty} (-y)^{-n+1} C_n(t, y^{-1}) s^{n\alpha(0) + \alpha't/n-n+1}. \quad (1.1)$$

The factor  $y^{-n+1}$  is predicted by Reggeon unitarity to be the leading behavior of the n-Reggeon cut, and the alternating signs appear in all models based on Feynman diagrams with even signature poles near  $\Delta = 0$ . Equation (1.1) is a useful asymptotic series only for  $\Delta < 0$ , but if it can be summed, the sum can be evaluated for  $\Delta > 0$ . One then

obtains the scattering amplitude for  $\Delta > 0$  provided--as we assume-- that no Stokes phenomenon occurs at  $\Delta = 0$ . In other words, we assume that the sum of terms that are subdominant for  $\Delta < 0$  remains subordinate for  $\Delta > 0$ . The Regge-eikonal model is an example of a model where the Regge cuts can be summed and then continued to  $\Delta > 0$  in this manner; the result is the black disk Pomeron. The chief defect of the Regge-eikonal model is that it ignores processes in which Reggeons split into several Reggeons. These are precisely the processes emphasized in the Reggeon calculus.

We shall calculate  $C_n(t, y^{-1})$  in the Reggeon calculus for  $\Delta > 0$ . To do so exactly we should have to calculate all diagrams, which is conceivable only for  $\Delta = 0$ . We are therefore forced to calculate in the weak coupling approximation, where unrenormalized  $p$  Reggeon vertices  $r_p$  are all small constants. We calculate the Regge cuts to lowest order in products of these constants. A typical diagram in the weak coupling class is shown in Fig. 1, where the dashed line indicates the discontinuity taken in the angular momentum plane, and  $\beta_p$  is the coupling of  $p$  Reggeons to external particles. The weak coupling class of diagrams has the property that the dashed line separates the diagram into two trees. We also require that  $r_p$  is of the same order of smallness as  $(r_3)^{p-2}$  so that diagrams with different kinds of couplings are of comparable strength.

Some approximations must be made to evaluate our diagrams. When

calculating the discontinuity across Regge cuts, we take the expression near the threshold of each cut and regard it as adequate down to the next cut to the left. Since the cut to the left has a discontinuity with lower powers of the  $r$ 's, the accuracy of the discontinuity matters only in this interval. This approximation is tantamount to replacing the  $C_n(t, y^{-1})$  by their asymptotic values  $C_n(t, 0)$ . We recognize there is no guarantee that the sum of the corrections, each suppressed by powers of  $y^{-1}$ , is subdominant to the sum we calculate. The approximation is an inevitable one in weak coupling approximations: The asymptotic behavior of the perturbation sum is assumed to be the sum of the asymptotic behaviors of the terms.

A second approximation is to ignore the  $t$ -dependence of the propagators in the tree production amplitudes of Fig. 1. As we shall see in Sec. II, this approximation is adequate for  $-\Delta \ll \alpha' t < 0$ . Since the  $t$ -variation of  $s^{\alpha' t/n}$  becomes more rapid as  $s$  increases, this approximation is harmless at high energies. This second approximation replaces  $C_n(t, 0)$  by  $C_n(0, 0)$  in Eq. (1.1).

In Sec. II we begin the calculation by assuming only  $\beta_1$  and one of the  $r_p$  are nonzero. We find an absorbing disk Pomeron satisfying unitarity for  $p = 3$ , but for  $p \geq 4$  the Froissart bound is violated. In Sec. III we explore the domain in the space of coupling constants where unitarity is satisfied by considering the case where  $r_3$  and  $r_4$  are nonzero. We find that unitarity is satisfied when  $W \equiv 2\Delta r_4 / 3r_3^2$  lies in the interval  $-\infty < W < 1/4$ . This suggests

that unitarity is satisfied if the higher couplings are small compared with  $r_3$ , or if they have the right sign. In Sec. IV we turn on all the  $\beta_p$ 's but take  $r_p = 0$  for  $p \geq 4$ . There we show that the leading asymptotic behavior factorizes even when there are direct couplings of particles to many Reggeons.

## II. SUMMATION OF CUTS WITH $\beta_1$ AND ONE $r_p$ NONZERO

Our first task is to count Reggeon production diagrams like those on one side of Fig. 1. We shall use Rayleigh-Schrodinger perturbation theory, so graphs which differ by order of emission of the Reggeons are distinct. One Reggeon is emitted by  $\beta_1$ , and each time  $r_p$  acts  $p-2$  additional Reggeons appear. When  $r_p$  occurs  $n$  times, the intermediate state has  $n(p-2) + 1$  Reggeons. We denote the number of such production amplitudes on one side by  $N_p(n)$ , which satisfies the recursion relation

$$N_p(n) = \frac{(n-1)! [n(p-2) + 1]!}{(p-1)!} \sum_{n_1=0}^{\infty} \dots \sum_{n_{p-1}=0}^{\infty} \delta(n-1, \sum_{i=1}^{p-1} n_i) \quad (2.1)$$

$$\times \prod_{j=1}^{p-1} \frac{N_p(n_j)}{n_j! [n_j(p-2) + 1]!}; \quad N_p(0) = 1.$$

This recursion relation is illustrated in Fig. 3, and the various terms can be understood as follows. The Kronecker delta requires the final number of Reggeons to be  $n(p-2) + 1$ , and the summations allow branch  $i$  to have any number of vertices  $n_i$ . The factor  $[n(p-2) + 1]! / \prod_{j=1}^{p-1} [n_j(p-2) + 1]!$

is the number of ways the produced Reggeons, which are labelled, can be allocated to the branches. The factor  $(n-1)!$  is the number of orders in which vertices subsequent to the first can occur, and the factors  $1/\prod_{j=1}^{p-1} n_j!$  are required because  $N_p(\mathbf{n}_j)$  already counts the number of orders of vertices within the  $j$ -th branch. The factor  $1/(p-1)!$  appears because diagrams differing by a reindexing of the branches are not distinct.

$N_p(n)$  is obtained from Eq. (2.1) by introducing the generating function

$$f_p(Z) = \sum_{n=0}^{\infty} \frac{N_p(n) Z^n}{n! [(p-2)n + 1]!}; f_p(0) = 1. \quad (2.2)$$

Equation (2.1) may be written

$$n \frac{N_p(n)}{n! [(p-2)n + 1]!} = \frac{1}{(p-1)!} \frac{1}{2\pi i} \oint \frac{dZ}{Z^n} [f_p(Z)]^{p-1}, \quad (2.3)$$

where the circuit encloses the origin but none of the singularities of  $f_p(Z)$ . Multiply this equation by  $X^{n-1}$  and sum on  $n$  from 1 to  $\infty$ .

$$f_p'(X) = \frac{1}{(p-1)!} \frac{1}{2\pi i} \oint \frac{dZ}{Z-X} [f_p(Z)]^{p-1} = \frac{1}{(p-1)!} [f_p(X)]^{p-1}. \quad (2.4)$$

The solution of this differential equation gives

$$N_p(n) = \left[ \frac{p-2}{(p-1)!} \right]^n \frac{[(p-2)n + 1]! \Gamma[n + 1/(p-2)]}{\Gamma[1/(p-2)]}. \quad (2.5)$$

The cut discontinuity shown in Fig. 1 can be evaluated using rules given in Ref. 2. When the discontinuity across the  $m$ -Reggeon cut is taken, we encounter a phase space integral



$$\begin{aligned} \mathbb{I}_m &= \int \left[ \prod_{i=1}^m \frac{d^2 q_i}{(2\pi)^2} \right] (2\pi)^2 \delta(\vec{k} - \sum_{i=1}^m \vec{q}_i) \delta[j-1 - \sum_{i=1}^m (\Delta - \alpha' q_i^2)] \\ &= \frac{m-1}{(4\pi\alpha')^{m-1} m!} \theta(m\Delta - j + 1 - \alpha't/m) (m\Delta - j + 1 - \alpha't/m)^{m-2}. \end{aligned} \quad (2.6)$$

The theta function determines the threshold of the  $m$ -Reggeon cut to be  $j = 1 + m\Delta + \alpha't/m$ ; at threshold each  $t_i = -q_i^2 = t/m^2$ . In the production amplitudes each Reggeon has angular momentum  $\alpha(t_i)$ . An intermediate state with  $c$  Reggeons produces an energy denominator  $[(j-1) - \sum_{i=1}^c (\Delta + \alpha't_i)]^{-1}$ . At the tip of the  $[(p-2)n + 1]$  Reggeon cut,  $j-1 = [(p-2)n + 1]\Delta + \alpha't/[(p-2)n + 1]$ , and  $-\sum_{j=1}^c \alpha't_j \leq -\alpha't$ . Thus each energy denominator is bounded by

$$\begin{aligned} \left\{ [(p-2)n + 1 - c]\Delta + \alpha't/[(p-2)n + 1] \right\}^{-1} &\geq \left\{ (j-1) - \sum_{i=1}^c (\Delta + \alpha't_i) \right\}^{-1} \\ &\geq \left\{ [(p-2)n + 1 - c]\Delta - \alpha't + \alpha't/[(p-2)n + 1] \right\}^{-1}. \end{aligned} \quad (2.7)$$

After  $q$  Reggeon emissions have occurred,  $c = [(p-2)q + 1]$ . If  $-\Delta \ll \alpha't < 0$ , as we assume, the denominator is very close to  $[(p-2)(n-q)\Delta]^{-1}$ . The product of all energy denominators in each production amplitude is therefore  $(p-2)^{-n} \Delta^{-n} (n!)^{-1}$ .

We have all elements required to write the sum of the cuts.<sup>5</sup>

$$\begin{aligned} \text{Im } M(s, t) &= \frac{\pi}{2} \beta_1^A \beta_1^B s^{1+\Delta+\alpha't} + \frac{p-2}{\Gamma^2[1/(p-2)]} \int_{-\infty}^{\infty} dj s^j \\ &\times \sum_{n=1}^{\infty} \frac{\Gamma^2[n+1/(p-2)]}{n!(n-1)!} \theta\{n(p-2)\Delta + \Delta - j + 1 + \alpha't/[n(p-2) + 1]\} \end{aligned}$$

$$\begin{aligned} & \times \left\{ n(p-2)\Delta + \Delta - j + 1 + \alpha't / [n(p-2) + 1] \right\}^{n(p-2) - 1} \\ & \times \left\{ \frac{r_p^2}{[(p-1)!]^2 \Delta^2 (-4\pi\alpha')^{p-2}} \right\}^n . \end{aligned} \tag{2.8}$$

In the n-th term let

$$\begin{aligned} X &= \left\{ n(p-2)\Delta + \Delta - j + 1 + \alpha't / [n(p-2) + 1] \right\} y, \\ Z &= \frac{r_p^2 s^{(p-2)}}{[(p-1)!]^2 \Delta^2 (-4\pi\alpha' y)^{p-2}} . \end{aligned} \tag{2.9}$$

Then

$$\begin{aligned} \text{Im } M(s, t) &= \frac{\pi}{2} \beta_1^A \beta_1^B s^{1+\Delta+\alpha't} + \frac{\pi}{2} \beta_1^A \beta_1^B \frac{(p-2)s^{1+\Delta}}{\Gamma^2[1/(p-2)]} \\ & \times \int_0^\infty \frac{dXe^{-X}}{X} \sum_{n=1}^\infty \frac{s^{\alpha't/[n(p-2)+1]} \Gamma^2[n+1/(p-2)]}{n!(n-1)!} (X^{p-2} Z)^n . \end{aligned} \tag{2.10}$$

At t=0 the sum is a hypergeometric function, for which we use the Mellin-Barnes integral. Interchanging order of integrations and evaluating the X-integral we find

$$\begin{aligned} \text{Im } M(s, 0) &= \frac{\pi}{2} \beta_1^A \beta_1^B s^{1+\Delta} + \frac{\pi}{2} \beta_1^A \beta_1^B \frac{(p-2)s^{1+\Delta} Z}{\Gamma^2[1/(p-2)]} \\ & \times \frac{1}{2\pi i} \int_{-\frac{1}{2}-i\infty}^{-\frac{1}{2}+i\infty} \frac{d\lambda}{\Gamma(\lambda+2)} \Gamma^2(\lambda+1+\frac{1}{p-2}) \Gamma[(p-2)(\lambda+1)] \Gamma(-\lambda)(-Z)^\lambda . \end{aligned} \tag{2.11}$$

The first two terms in the large  $Z$  expansion of the Mellin-Barnes integral are given by the simple pole at  $\lambda = -1$  and, for  $p \geq 4$ , by the triple pole at  $\lambda = -1-1/(p-2)$ . The contribution of the pole at  $\lambda = -1$  cancels the single Reggeon exchange term, leaving the asymptotic expression

$$\text{Im } M(s, 0) \sim \pi \beta_1^A \beta_1^B s y^3 \Delta^2 (p-2) \left\{ \frac{[(p-1)!]^2 \Delta^2}{(-1)^{p-1} r_p^2} \right\}^{\frac{1}{p-2}} \alpha' \sin \frac{\pi}{p-2}. \quad (2.12)$$

( $p \geq 4$ )

The total cross sections predicted by Eq. (2.12) are real only when  $p$  is odd; even then they violate the Froissart bound by one power of  $y$ .

For  $p=3$ , the triple pole is reduced to a double pole. We find the asymptotic behavior

$$\text{Im } M(s, 0) \sim \frac{8\pi^2 \Delta^3 \alpha' \beta_1^A \beta_1^B s y^2}{r_3^2}. \quad (2.13)$$

The corresponding cross sections have the energy dependence of the Froissart bound. The next lower power in the cross section is the term  $s^{1-\Delta} y^3$ , so in this calculation the parameter  $\Delta$  is directly related to subasymptotic powers in total cross sections. A similar phenomenon occurs in the Regge-eikonal model.

The constraint of unitarity can be explored further, for  $p=3$ , by examining the  $s$ -channel partial-wave amplitude in the impact parameter formulation.

$$\text{Im } f(s, b) = \frac{1}{s} \int_{-\infty}^0 dt J_0(b\sqrt{-t}) \text{Im } M(s, t). \quad (2.14)$$

Inserting Eq. (2.10) and summing on  $n$ ,

$$\text{Im} f(s, b) = \frac{8\pi^2 \Delta^2}{r_3^2} \beta_1^A \beta_1^B \left\{ 1 - \int_0^\infty \frac{dX e^{-X}}{1 + \frac{X r_3^2 \Delta^2 e^{-b^2/4\alpha'y}}{16\pi\alpha'y\Delta^2}} \right\} \quad (2.15)$$

$\text{Im} f(s, b)$  is positive for elastic scattering and decreases monotonically to zero as  $b$  increases. Thus, if  $(\beta_1)^2$  is not too large, the unitarity bound on elastic amplitudes,  $0 \leq \text{Im} f(s, b) \leq 1$ , is satisfied. For large  $s$ , the brace in Eq. (2.15) becomes nearly a theta function  $\theta(2y\sqrt{\alpha'\Delta} - b)$  with a radius proportional to  $y$ . The radius is related to  $\alpha'$  and  $\Delta$  in the same way in the Regge-eikonal model. The width of the edge of the disk remains finite as  $s \rightarrow \infty$ . This factorizing, uniformly absorbing Pomeronanchon disk is described in the  $t$ -channel as a pair of trajectories

$$\alpha_\pm(t) = 1 \pm 2\sqrt{\alpha'\Delta t}. \quad (2.16)$$

### III. SUMMATION OF CUTS WITH $\beta_1$ , $r_3$ AND $r_4$ NONZERO

In Sec. II we summed Reggeon cuts to obtain an unitary amplitude, but only for  $p=3$ . In general, all  $r_p$ 's will be finite, and then we need to know the domain in the space of coupling constants where unitarity is satisfied. In this Section we study a simple section of this domain by taking  $r_3$  and  $r_4$  to be finite. We show that the amplitude is unitary if  $r_3$  is the dominant coupling, or if  $r_4$  is negative. When one of these conditions is satisfied, the amplitude resembles Eqs. (2.13) and (2.15).

We begin by counting the number of Reggeon production diagrams in which  $n+1$  Reggeons are produced, with all vertices triple Regge vertices except the last, which is a four Regge vertex. The number of such diagrams is

$$N_{\alpha}(n) = N_3(n-2) \frac{(n+1)!}{(n-2)!3!} = \frac{2}{3n} N_3(n), \quad (3.1)$$

where the combinatorial factor counts the number of ways of allocating the Reggeons to the vertices.

Next we count the number of diagrams in which  $n_1+1$  labelled Reggeons are increased to  $n+1$  labelled Reggeons by means of emissions at triple Regge vertices. The number of such diagrams,  $N_{\beta}(n_1, n)$ , satisfies

$$N_3(n_1) \frac{1}{(n_1+1)!} N_{\beta}(n_1, n) = N_3(n) \quad (3.2)$$

Combining  $N_{\alpha}$  and  $N_{\beta}$ , we calculate the number of diagrams leading to  $n+1$  Reggeons, with just one four Reggeon vertex acting before the intermediate state with  $n_1+1$  Reggeons. This is

$$\begin{aligned} N_{3,4}(n; n_1) &= N_{\alpha}(n_1) \frac{1}{(n_1+1)!} N_{\beta}(n_1, n) \\ &= \frac{2}{3n_1} N_3(n). \end{aligned} \quad (3.3)$$

Continuing in this way, we determine the number of diagrams with  $n+1$  final Reggeons, and with four Regge vertices before intermediate states with  $n_1+1, n_2+1, \dots$  Reggeons.

$$N_{3,4}(n; n_1, n_2, \dots) = N_3(n) \prod_{i=1} \frac{2}{3n_i} \quad (3.4)$$

The values of diagrams with four Regge vertices at locations  $n_1$ ,  $n_2$ , ... are simple modifications of the result in Sec. III. A multiplicative factor  $r_4/r_3^2$  occurs due to the replacement of two triple Regge vertices by one four Regge vertex. Also, the energy denominator  $[(n+1-n_1)\Delta]^{-1}$  is omitted. Equation (2.10) becomes

$$\begin{aligned} \text{Im } M(s, t) &= \frac{\pi}{2} \beta_1^A \beta_1^B s^{1+\Delta+\alpha't} + \frac{\pi}{2} \beta_1^A \beta_1^B s^{1+\Delta} \int_0^\infty \frac{dX e^{-X}}{X} \\ &\times \sum_{q_1=0}^\infty \sum_{q_2=0}^\infty W^{q_1+q_2} \sum_{n=\max(1, 2q_1, 2q_2)}^\infty C(n, q_1) C(n, q_2) m s^{\alpha't/(n+1)} (XZ)^n. \end{aligned} \quad (3.5)$$

Here  $W \equiv 2 \Delta r_4 / 3 r_3^2$  is finite in the weak coupling limit, and

$$C(n, q) = \sum_{n_q=2q}^n \frac{n+1-n_q}{n_q} \sum_{n_q=2(q-1)}^{n_q-2} \frac{n+1-n_{q-1}}{n_{q-1}} \dots \sum_{n_1=2}^{n_2-2} \frac{n+1-n_1}{n_1}; \quad (3.6)$$

$$C(n, 0) = 1$$

The sums in  $C(n, q)$  distribute  $q$  four Regge vertices in the production amplitudes in all possible ways. Integrate Eq. (3.5) by parts. The single Reggeon exchange term can be absorbed into the sum, and we have

$$\begin{aligned} \text{Im } M(s, 0) &= \frac{\pi}{2} \beta_1^A \beta_1^B s^{1+\Delta} \int_0^\infty dX e^{-X} F(XZ, W), \\ \text{Im } f(s, b) &= \frac{8 \pi^2 \Delta^2 \beta_1^A \beta_1^B}{r_3^2} (-Z') \int_0^\infty dX e^{-X} X F(XZ', W), \end{aligned} \quad (3.7)$$

where  $Z' = e^{-b^2/4\alpha'y} Z$ , and

$$F(Z, W) = \sum_{q_1=0}^{\infty} \sum_{q_2=0}^{\infty} W^{q_1+q_2} \sum_{n=2 \max(q_1, q_2)}^{\infty} C(n, q_1) C(n, q_2) Z^n. \quad (3.8)$$

To study  $F$ , we first generalize  $C(n, q)$  to  $C(n, m, q)$ .

$$C(n, m, q) = \sum_{n_q=2q}^m \frac{n+1-n_q}{n_q} \sum_{n_{q-1}=2(q-1)}^{n_q-2} \frac{n+1-n_{q-1}}{n_{q-1}} \dots \sum_{n_1=2}^{n_2-2} \frac{n+1-n_1}{n_1}, \quad (3.9)$$

$$C(n, m, 0) = 1 .$$

Thus,  $C(n, n, q) = C(n, q)$ . The new coefficients satisfy the recursion relation

$$C(n, m, q) = C(n, m+1, q) - \frac{n-m}{m+1} C(n, m-1, q-1). \quad (3.10)$$

Introduce the generating function

$$G(n, Z, W) = \sum_{q=0}^{\infty} \sum_{m=2q}^{\infty} C(n, m, q) Z^m W^q. \quad (3.11)$$

Equation (3.10) implies that  $G$  satisfies the differential equation and boundary condition

$$\left\{ (1-Z+WZ^2) \frac{\partial}{\partial Z} - [(n-1)WZ + 1] \right\} G(n, Z, W) = 0, \quad (3.12)$$

$$G(n, 0, W) = 1 .$$

The solution is

$$G(n, Z, W) = [A(Z, W)]^{n+1} [B(Z, W)]^{n-1}, \quad (3.13)$$

where

$$A(Z, W) = \left[ \frac{(1 + \sqrt{1-4W} - 2WZ)(1 - \sqrt{1-4W})}{(1 - \sqrt{1-4W} - 2WZ)(1 + \sqrt{1-4W})} \right]^{\frac{1}{2\sqrt{1-4W}}}, \quad (3.14)$$

$$B(Z, W) = (1 - Z + WZ^2)^{\frac{1}{2}}.$$

To get closer to F, consider the second generating function

$$\begin{aligned} G(Z, W) &= \sum_{q=0}^{\infty} \sum_{n=2q}^{\infty} C(n, n, q) Z^n W^q = \sum_{n=0}^{\infty} \frac{Z^n}{n!} \left. \frac{\partial^n}{\partial Z'^n} G(n, Z', W) \right|_{Z'=0} \\ &= \sum_{n=0}^{\infty} \frac{Z^n}{n!} \left. \frac{\partial^n}{\partial Z'^n} \left\{ \frac{A(Z', W)}{B(Z', W)} [A(Z', W)B(Z', W)]^n \right\} \right|_{Z'=0}. \end{aligned} \quad (3.15)$$

The sum may be evaluated by means of Lagrange's theorem.<sup>6</sup>

$$G(Z, W) = \frac{\phi(Z)}{Z[1 - \phi(Z)]}, \quad (3.16)$$

where  $\phi(Z)$  is the unique solution of the functional equation

$$\phi(Z) = ZA(\phi(Z), W)B(\phi(Z), W) \quad (3.17)$$

satisfying the boundary condition  $\phi(0) = 0$ . The function we want is related to  $G(Z, W)$  by

$$F(Z, W) = \frac{1}{2\pi i} \oint \frac{d\xi}{\xi} G(\xi Z, W)G\left(\frac{1}{\xi}, W\right), \quad (3.18)$$

where the contour runs inside the singularities of  $G(\xi Z, W)$  and outside the singularities of  $G(\frac{1}{\xi}, W)$ .

To use Eqs. (3.16-19), we must determine the properties of  $\phi(Z)$ . For this purpose, consider the inverse function

$$Z(\phi) = \frac{\phi}{A(\phi, W)B(\phi, W)}. \quad (3.19)$$



We immediately note that  $Z(\phi)$  is infinite when A or B vanishes, i. e.,

at  $\phi = \phi_{\pm}$ :

$$\phi_{\pm} = \frac{1 \pm \sqrt{1-4W}}{2W} . \tag{3.20}$$

Therefore, on every sheet  $\phi(Z)$  must approach one of  $\phi_{\pm}$  as  $Z \rightarrow \infty$ .

$Z(\phi)$  possesses an analytic inverse  $\phi(Z)$  except where  $Z(\phi)$  is singular,

or where

$$\frac{dZ}{d\phi} = \frac{Z(\phi)(1-\phi)}{\phi(1-\phi+W\phi^2)} \tag{3.21}$$

vanishes. Possible singular values of  $\phi$  are thus  $\phi = 1, \phi_{\pm}$  or  $\infty$ . The

corresponding possible singular points of  $\phi(Z)$  can be gotten from

Eq. (3.19); depending on W they are  $Z = Z_0$ ; 0 or  $\infty$ ;  $Z_1$ .

$$Z_0 = \frac{1}{A(1, W)B(1, W)}, \quad Z_1 = \lim_{Z \rightarrow \infty} \frac{Z}{A(Z, W)B(Z, W)}. \tag{3.22}$$

The formulas for  $Z_0$  and  $Z_1$  are multivalued, and any branch can be a singular point on some sheet of  $\phi(Z)$ . According to Lagrange's theorem, we are interested in the sheet of  $\phi(Z)$  where  $\phi(0) = 0$  and  $\phi(Z)$  is analytic at  $Z = 0$ ; cuts in the Z-plane are to be drawn from singular points to infinity. Therefore,  $Z = 0$  is not a singular point of  $\phi(Z)$  and  $G(Z, W)$  on the sheet of interest here. By expanding Eq. (3.19) about  $\phi = \infty$ , it can be seen that  $\phi(Z)$  has a simple pole at  $Z = Z_1$ . According to Eq. (3.16), this does not produce a singularity of  $G(Z, W)$ , so the only finite singularities of  $G(Z, W)$  are at one or more of the branches of  $Z_0$ .

The next step is to determine which branches of  $Z_0$  are singularities of  $\phi(Z)$ . The results depend on W, and we first take the case  $0 < W < \frac{1}{4}$ .

Consider the circuit in the  $\phi$ -plane illustrated in Fig. 4a. Equation (3.19) maps this into the circuit in the  $Z$ -plane shown in Fig. 4b; the circuit encloses the upper half  $Z$ -plane. Since the circuit in Fig. 4a can be continuously deformed to the origin without crossing any singularities of the mapping,  $|Z_0|$ ,  $-|Z_1|$  and  $\infty$  are the only singularities of  $\phi(Z)$  within or on the edge of the upper half plane. Consideration of the complex-conjugate to the path of Fig. 4a shows that  $|Z_0|$  is the only finite branch point of  $\phi(Z)$  in the cut  $Z$ -plane, and that the discontinuity of  $\phi(Z)$  across the cut drawn from  $|Z_0|$  to infinity is positive definite.  $\phi(\infty) = \phi_+$  in the cut plane. By expanding Eq. (3.19) around  $\phi = \phi_+$ , we find the discontinuity decreases like  $Z^{-\frac{2\sqrt{1-4W}}{1+\sqrt{1-4W}}}$  at large  $Z$ .

Equation (3.16) indicates that  $G(Z, W)$  is analytic except for a cut drawn from  $|Z_0|$  to  $\infty$ . The discontinuity is positive definite and has the same asymptotic power as the discontinuity of  $\phi(Z)/Z$ . We may therefore write the dispersion relation

$$G(Z, W) = \frac{1}{\pi} \int_{|Z_0|}^{\infty} \frac{dZ' p(Z')}{Z' - Z}, \quad p(Z) > 0. \quad (3.23)$$

Considering asymptotic behavior, we have

$$\phi_- = -\frac{\phi_+}{1 - \phi_+} = \frac{1}{\pi} \int_{|Z_0|}^{\infty} dZ' p(Z'). \quad (3.24)$$

Substituting into Eq. (3.18),

$$F(Z, W) = \frac{1}{\pi} \iint_{|Z_0|}^{\infty} \frac{dZ_1 dZ_2 p(Z_1) p(Z_2)}{Z_1 Z_2 - Z}, \quad (3.25)$$

$$F(Z, W) \underset{Z \rightarrow \infty}{\sim} \frac{(\phi_-)^2}{(-Z)}.$$

Equation (3.7) now gives the asymptotic behavior

$$\text{Im } M(S, 0) \sim \frac{8\pi^2 \Delta^3 \alpha'}{r_3^2} \beta_1^A \beta_1^B \text{sy}^2 \left[ \frac{1-2W-\sqrt{1-4W}}{2W^2} \right]. \quad (3.26)$$

This amplitude is unitary and differs from Eq. (2.13) only by the last factor, which approaches 1 at  $W=0$ .

It follows from Eq. (3.25) that the imaginary part of the s-channel partial wave amplitude is positive and decreases monotonically to zero as  $b$  increases indefinitely. At high  $s$  the Pomeron is again a uniform absorbing disk:

$$\text{Im } f(s, b) \sim \frac{8\pi^2 \Delta^2}{r_3^2} \beta_1^A \beta_1^B \left[ \frac{1-2W-\sqrt{1-4W}}{2W^2} \right] \theta(2y\sqrt{\alpha'\Delta} - b). \quad (3.27)$$

Altogether, when  $W$  is between 0 and  $1/4$ , no significant change is seen in the amplitude. For  $W > 1/4$ , the right side of Eq. (3.26) is complex and thereby violates unitarity.

The analysis for  $-\infty < W < 0$  is more complicated, and we only give results. The new feature is that  $\phi(Z)$  and  $G(Z, W)$  have branch points at  $|Z_0| e^{\pm i\psi}$ ,

$$\psi = \frac{\pi}{2} \left[ 1 - \frac{1}{\sqrt{1-4W}} \right]. \quad (3.28)$$

The dispersion relation for  $G(Z, W)$  is

$$G(Z, W) = \frac{i}{\pi} \int_{|Z_0|}^{\infty} dr R(r) \left[ \frac{1}{re^{i\psi} - Z} - \frac{1}{re^{-i\psi} - Z} \right], \quad (3.29)$$

where  $R(r) > 0$  and  $R(r)$  has the asymptotic behavior

$$R(r) \underset{r \rightarrow \infty}{\sim} \frac{\sqrt{1-4W}}{(-2Wr)}. \quad (3.30)$$

We also have

$$F(Z, W) = \frac{1}{\pi} \iint_{|Z_0|}^{\infty} dr_1 dr_2 R(r_1)R(r_2) \left[ \frac{2}{r_1 r_2 - Z} - \frac{1}{r_1 r_2 e^{2i\psi} - Z} - \frac{1}{r_1 r_2 e^{-2i\psi} - Z} \right]. \quad (3.31)$$

With the aid of Eq. (3.30), we find the asymptotic behavior

$$F(Z, W) \sim \begin{cases} \frac{(\phi_-)^2}{(-Z)} \left[ -\frac{\pi}{\sqrt{1-4W}} < \arg(-Z) < \frac{\pi}{\sqrt{1-4W}} \right] & (3.32a) \\ \frac{(\phi_-)^2 + (\phi_+)^2}{(-2Z)} + \frac{i(1-4W)\ell n(-Z)}{2\pi W^2(-Z)} + \frac{iC}{(-Z)} & \left[ \frac{\pi}{\sqrt{1-4W}} < \arg(-Z) < \pi \right] \end{cases} \quad (3.32b)$$

The complex conjugate to Eq. (3.32b) holds for  $-\pi < \arg(-Z) < -\frac{\pi}{\sqrt{1-4W}}$ ,

and  $C$  is an undetermined constant. It follows from Eq. (3.32a) that

Eqs. (3.26) and (3.27) continue to hold. However, the monotonicity of

$\text{Im } f(s, b)$  can no longer be established for  $-\infty < W < 0$ , which means we cannot rule out a local excursion of  $\text{Im } f(s, b)$  below zero near the edge of the disk. There is no reason to believe such an excursion occurs, but if it does, it constitutes a violation of unitarity over a limited range of impact parameters.

These results show no trace of the complex cross section which must appear in the limit of pure four Regge couplings. However, when  $s$  approaches infinity along a complex ray so that Eq. (3.32b) holds, we have

$$\text{Im } M(s, 0) \sim - \frac{12\pi i \beta_1^A \beta_1^B s y^3 \Delta^3 \alpha'}{r_4} \left( \frac{1-4W}{-4W} \right) . \quad (3.33)$$

In the limit  $W \rightarrow \infty$  this agrees with the complex cross section of Eq. (2.12).

#### IV. SUMMATION OF CUTS WITH $r_3$ AND ALL $\beta_p$ NONZERO

The results of Sec. III encourage us to conjecture that when  $r_3$  numerically dominates the other  $r_p$ , or possibly when the  $r_p$  have the proper sign, an unitary amplitude typical of pure triple Regge coupling emerges. Here we adopt this conjecture and put all the  $r_p$  ( $p \neq 3$ ) equal to zero. However, we now keep all the  $\beta_p$  finite. We shall see that the leading behavior of the forward imaginary amplitude is again  $sy^2$ , with a factorizing residue. It is quite unexpected for there to be factorization in the presence of direct couplings of many Reggeons to the external particles.

We calculate the sum of cuts associated with p Reggeons coupled to particle A, q Reggeons coupled to particle B, and interactions among the Reggeons due to  $r_3$ . The number of diagrams on the left leading to the production of n+1 Reggeons is  $[p!]^{-1} N_\beta(p-1, n)$ , and the value of each diagram is  $[\Delta^{n-p+1} (n-p+1)!]^{-1}$ . These are the only modifications of our previous formulas, and we obtain a contribution

$$\begin{aligned} \text{Im } M_{p,q}(s,t) &= \frac{\pi}{2} s^{1+\Delta} \left[ \frac{\beta_p^A}{p!(p-1)!} \left( \frac{2\Delta}{r_3} \right)^{p-1} \right] \left[ \frac{\beta_q^B}{q!(q-1)!} \left( \frac{2\Delta}{r_3} \right)^{q-1} \right] \\ &\times \int_0^\infty dX e^{-X} \sum_{n=\max(p,q)-1} s^{\alpha' t/(n+1)} \frac{n!}{(n-p+1)!} \frac{n!}{(n-q+1)!} (XZ)^n. \end{aligned} \tag{4.1}$$

At t=0 we obtain

$$\begin{aligned} \text{Im } M_{p,q}(s,0) &= \frac{\pi}{2} s^{1+\Delta} \left[ \frac{\beta_p^A}{p!(p-1)!} \left( \frac{2\Delta}{r_3} \right)^{p-1} \right] \left[ \frac{\beta_q^B}{q!(q-1)!} \left( \frac{2\Delta}{r_3} \right)^{q-1} \right] \\ &Z^{p-1} \left( \frac{\partial}{\partial Z} \right)^{p-1} Z^{q-1} \left( \frac{\partial}{\partial Z} \right)^{q-1} \int_0^\infty \frac{dX e^{-X}}{1-ZX}. \end{aligned} \tag{4.2}$$

Summing on p and q and taking the leading asymptotic behavior,

$$\text{Im } M(s,0) \sim \frac{8\pi^2 \Delta^3 \alpha' s y^2}{r_3^2} \left[ \sum_{p=1}^\infty \frac{\beta_p^A}{p!} \left( -\frac{2\Delta}{r_3} \right)^{p-1} \right] \left[ \sum_{q=1}^\infty \frac{\beta_q^B}{q!} \left( -\frac{2\Delta}{r_3} \right)^{q-1} \right]. \tag{4.3}$$

The factorization exhibited above does not hold for the term sy, which is down from the leading term only by y. This can be understood by examining the s-channel partial wave amplitude,  $\text{Im } f(s,b)$ .  $\text{Im } f(s,b)$  is

very nearly a theta function of radius  $2y\sqrt{\alpha'\Delta}$  and factorizing height. However, at the edge of the disk  $\text{Im } f(s, b)$  deviates from a perfect step by a contribution which does not factorize. This annulus of radius  $2y\sqrt{\alpha'\Delta}$  and finite width in impact parameter makes a contribution  $sy$  which does not factorize.

## V. CONCLUSIONS

It is surprising that the Reggeon calculus makes sense for  $\Delta > 0$ . We have found that only weak constraints must be placed on the Regge couplings to enforce  $s$  channel unitarity, and that the Pomeranchon is then an uniform absorbing disk of factorizing height in impact parameter space. This Pomeranchon is similar to the Regge-eikonal Pomeranchon except that it is only partially absorbing. Physically, it is more difficult to understand a partially absorbing disk than a black disk leading to equal asymptotic cross sections: The latter occurs when the absorption becomes large regardless of how the absorption arises. More will be known about how our cross section is built up when multiparticle final states are studied.

The multiple scattering series further emphasizes the difference between the Reggeon calculus model and the Regge-eikonal model. In the version studied in Sec. IV, the multiple scattering series for the Reggeon calculus model has coefficients

$$\begin{aligned}
 C_n(0,0) = & \frac{8\pi^2 \alpha' \Delta^2}{r_3^2} n! \left( \frac{r_3^2}{16\pi \alpha' \Delta^2} \right)^n \left[ \sum_{p=1}^n \frac{n!}{(n-p+1)!} \frac{\beta_p^A}{p!(p-1)!} \right. \\
 & \left. \times \left( \frac{2\Delta}{r_3} \right)^{p-1} \right] \left[ \sum_{q=1}^n \frac{n!}{(n-q+1)!} \frac{\beta_q^B}{q!(q-1)!} \left( \frac{2\Delta}{r_3} \right)^{q-1} \right].
 \end{aligned}
 \tag{5.1}$$

The Regge-eikonal model has

$$C_n(0,0) = \left[ \frac{\pi \beta_1^A \beta_1^B}{\alpha'} \right] \frac{\alpha'}{2n(n!)} \tag{5.2}$$

In the Reggeon calculus model the multiple scattering series is not convergent due to  $n!$ , although it is Borel summable. (The Sommerfeld-Watson integral is the Borel sum.) The factor  $n!$  is attributable to the huge number of Reggeon branching diagrams, which are absent in the Regge-eikonal model. The sum of the cuts is unitary for arbitrary  $\beta_p$  precisely because these splittings are present. On the other hand, the eikonal model has a convergent multiple scattering series. The model enforces unitarity by relating  $\beta_p$  to  $\beta_1$  in a special way.

#### ACKNOWLEDGMENTS

It is a pleasure to acknowledge the hospitality of the University of California at Santa Barbara, where part of this research was carried out.



REFERENCES

- <sup>1</sup>C. Edward Jones, F. E. Low, S. -H. H. Tye, G. Veneziano, and J. E. Young, Phys. Rev. D6, 1033 (1972).
- <sup>2</sup>V. N. Gribov, Zh. Eksp. Teor. Fiz. 53, 654 (1967) [Sov. Phys. - JETP 26, 414 (1968)].
- <sup>3</sup>M. Gell-Mann and Y. Ne'eman, The Eightfold Way (W. A. Benjamin, Inc., New York, 1964), p. 198.
- <sup>4</sup>H. Cheng and T. T. Wu, Phys. Rev. Letters 24, 1456 (1970); S.-J. Chang and T. -M. Yan, ibid., 25, 1586 (1970).
- <sup>5</sup>A factor  $1/[(p-2)n + 1]!$  is inserted on account of the identity of the Reggeons in the discontinuity. This automatically inserts a factor  $1/q!$  in graphs where  $q$  Reggeons emitted at one vertex on the left are absorbed at one vertex on the right. Such boson counting factors originate in the underlying field theory.
- <sup>6</sup>E. T. Whittaker and G. N. Watson, Modern Analysis (Cambridge University Press, 1958), p. 133.

FIGURE CAPTIONS

- Fig. 1                    A contribution to the five-Reggeon cut discontinuity  
in the weak coupling approximation.
- Fig. 2                    A correction to Fig. 1 which is excluded in the  
weak coupling approximation.
- Fig. 3                     $N_p(n)$  is built up as a sequence of branchings.
- Fig. 4a                  Circuit in  $\phi$  plane. Values of  $\phi$  at A, B, C are  
 $1, \phi_-, \phi_+$ . The semicircle D has a very large  
radius.
- Fig. 4b                  The mapping of Fig. 4a in the Z plane by Eq. (3.19).  
The singularity at  $-|Z_1|$  is a simple pole.

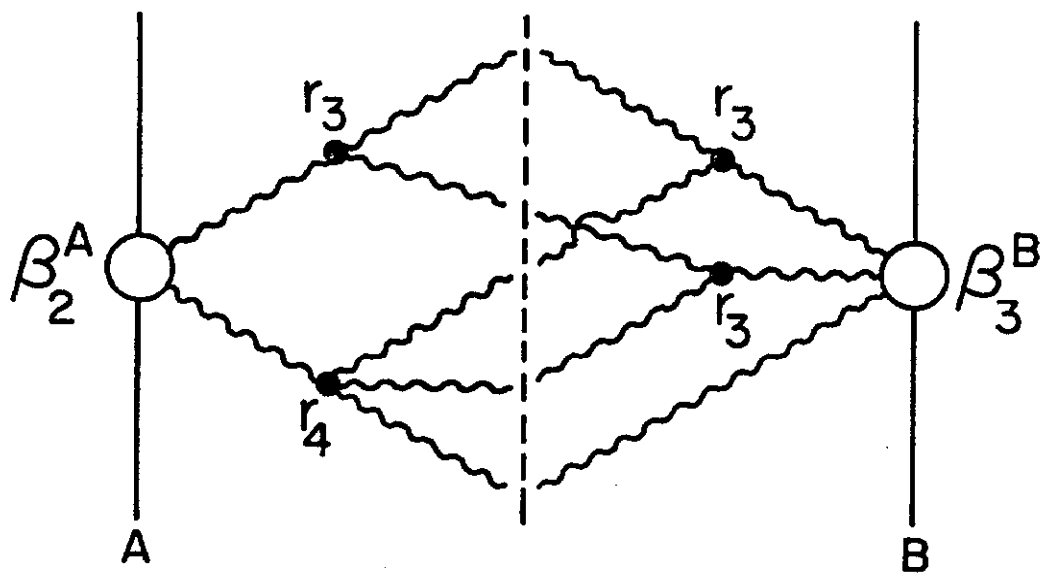


FIG. 1

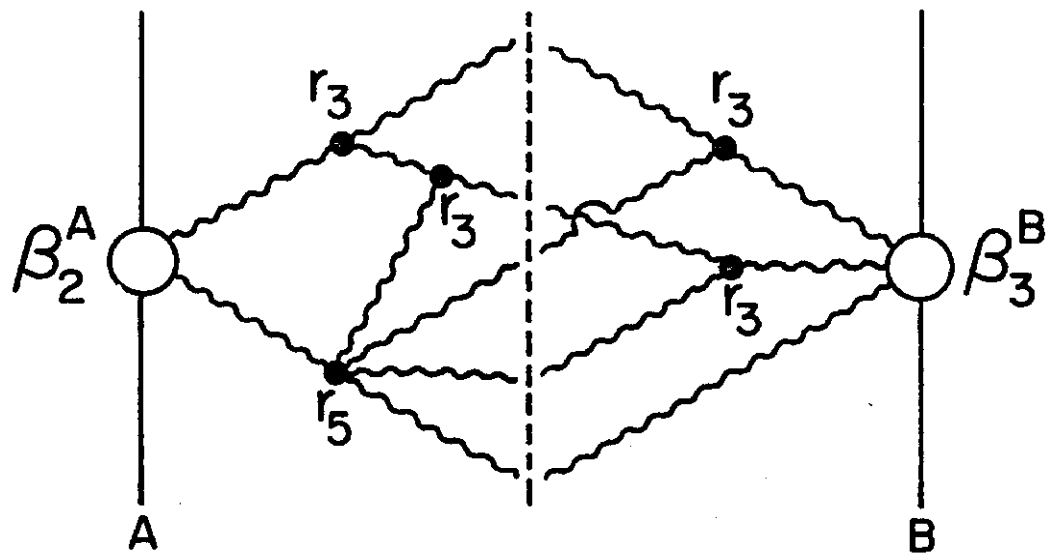


FIG. 2

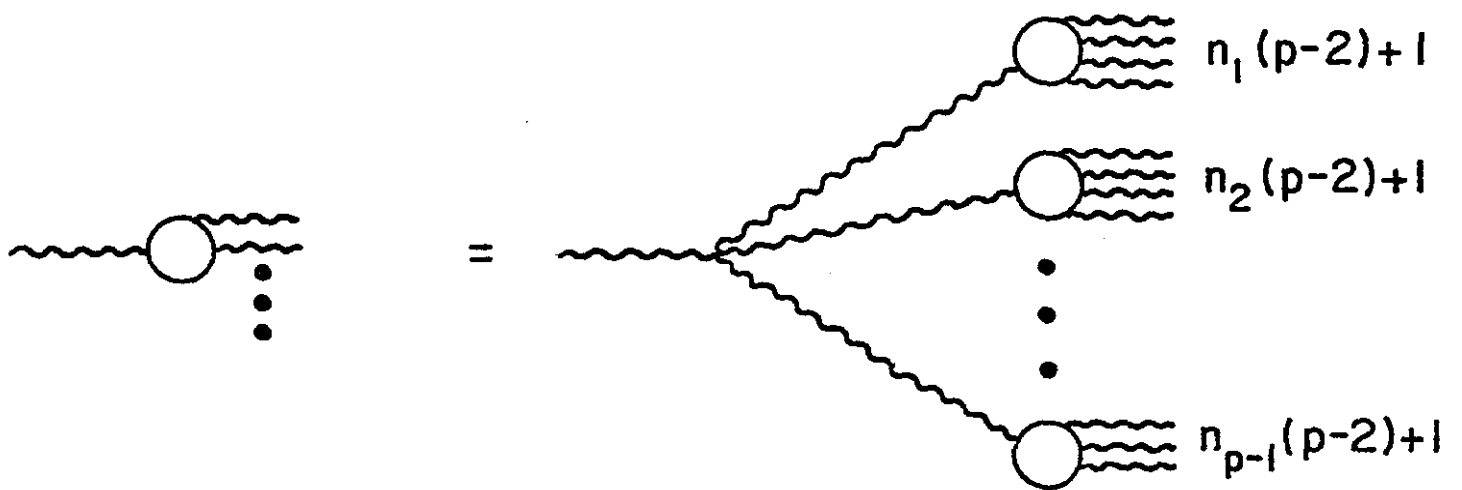


FIG. 3

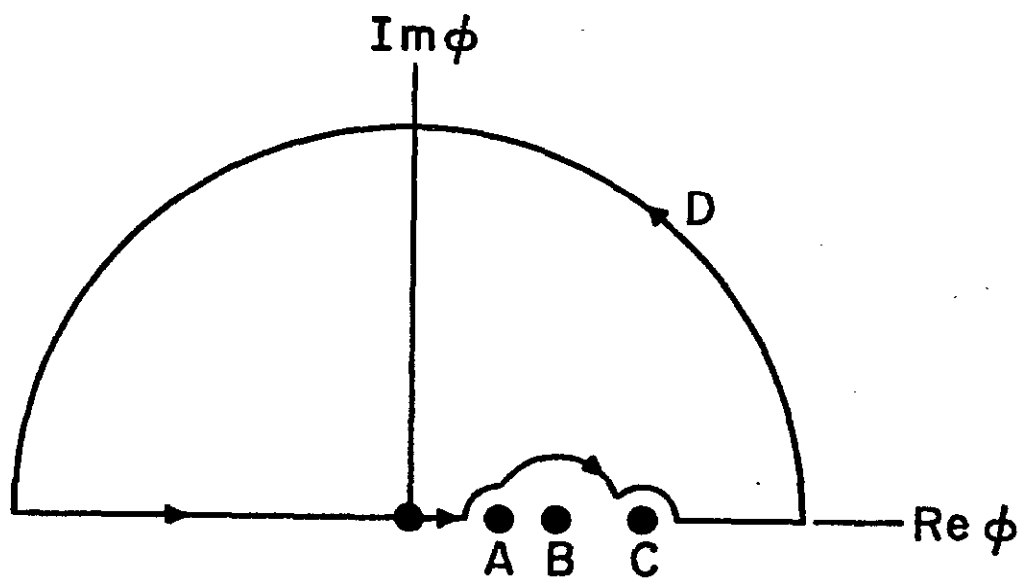


FIG. 4 (a)

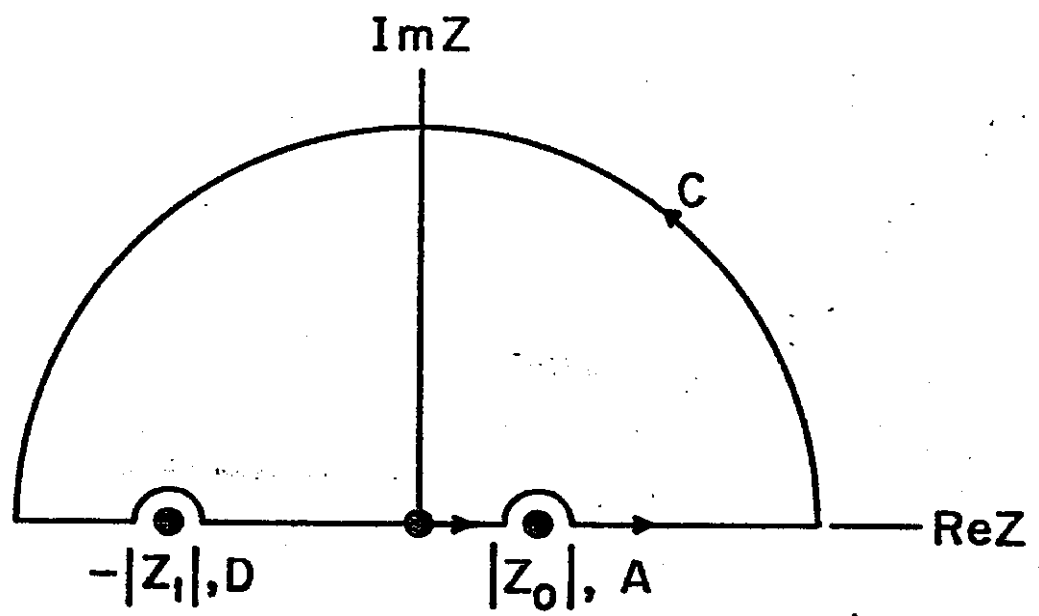


FIG. 4(b)